Bull. Inst. Chem. Res., Kyoto Univ., Vol. 70, No. 2, 1992

REVIEW

Dynamics of Polymers in the Bulk State by Neutron Scattering

Toshiji KANAYA*, Keisuke KAJI*, Tatsuya KAWAGUCHI* and Kazuhiko INOUE**

Received June 16, 1992

Dynamics of polymers in the bulk state was studied by quasi- and inelastic neutron scattering techniques in the time range of 10^{-13} to 10^{-10} s. The present work can be classified into three parts: (i) dynamics in the glassy state, (ii) dynamics near the glass transition and (iii) dynamics in the molten state. In the first section, we discuss the *low energy excitation* in glassy polymers, which is an origin of anomalous thermal properties of amorphous materials at low temperatures. In the next section, we study dynamics of amorphous polymers near the glass transition which is one of the current topics of solid state physics as well as polymer physics. It was found that two modes of motion appear near the glass transition in the energy ranges near 1 meV and of 10–30 μeV. These fast and slow modes arising ca. 50K below T_g and just above T_g, respectively, are discussed from viewpoints of molecular basis. In the last section, dynamics in the molten state is investigated by focusing on the mechanism of local conformational transition of polymer chains. The results are analyzed in terms of jump diffusion model with damped vibrational motions and compared with the Kramers' rate theory.

KEYWORDS: Dynamics/Amorphous Polymers/Low Energy Excitation/Glass Transition/ Damped Vibration/Conformational Transition/Neutron Scattering/

1. INTRODUCTION

Dynamics of polymer chains has been investigated by many techniques[1] such as mechanical relaxation, ultrasonic attenuation, dielectric relaxation, dynamic light scattering, fluorescence depolarization and NMR. Polymer motions slower than 10^{-6} s are now well understood in terms of Rouse model[2], which are strongly related to the so-called segmental motions. Recently, the tube model[3] has shed light on the substantial nature of very slow motions in entangled systems. However, there remain a lot of unsolved problems in motions faster than 10^{-8} s in spite of much efforts made by many research groups[4]. Less understood are very local motions especially in the time range of 10^{-13} to 10^{-10} s because there are few methods to access this time range, which is in the boundary between periodic motions (oscillatory motions) and relaxation motions, so that studies in this time range are fundamental to understand relaxation processes in polymer systems from microscopic view-

* 金谷利治，梶　慶輔，川口辰也：Institute for Chemical Research, Kyoto University, Uji, Kyoto-fu 611

** 井上和彦：Department of Nuclear Engineering, Hokkaido University, Sapporo, Hokkaido 060

points. Neutron scattering is one of the most valuable and powerful tools to study the motion in such time range.

In the present paper, we review our recent experimental results concerning dynamics of polymers in the bulk state studied by quasi- and inelastic neutron scattering techniques in the time range of 10^{-13} to 10^{-10} s. Our studies can be for convenience classified into three parts; (i) dynamics in the glassy state, (ii) dynamics near the glass transition and (iii) dynamics in the molten state though these three subjects are strongly related to each other. In each section, we will give a brief introduction to clarify the problems in each subject.

2. Neutron Scattering Measurements

Quasi- and inelastic neutron scattering measurements were performed with the inverted time-of-flight (TOF) spectrometers LAM-40[5] and LAM-80[5,6] installed at the pulsed spallation cold neutron source in the National Laboratory for High Energy Physics (KEK), Tsukuba. In operation of the spectrometers, pulsed cold neutrons with a wide energy distribution are incident on a sample and the scattered neutrons with fixed energy (4.59 meV and 1.8 meV for LAM-40 and LAM-80, respectively) are selected by a PG(002) or mica(006) crystal analyzer mirrors and Be filter and detected by ^{3}He counters at several scattering angles. The energy resolutions evaluated from the full width of the elastic peak are ca. 0.2 and ca. 0.018 meV, and the energy window are below 10 and 0.5 meV, respectively. The length of the scattering vector Q at the elastic position ranges from 0.2 to 2.6 $Å^{-1}$ and from 0.2 to 1.8 $Å^{-1}$ for LAM-40 and LAM-80, respectively.

The observed TOF spectrum was converted to dynamic scattering law $S(Q,\omega)$ and/or density of states $G(\omega)$ after making corrections for background, counter efficiency, and the incident neutron spectrum. The observed dynamic scattering law $S(Q,\omega)$ can be approximated to the incoherent dynamic scattering law because polymers measured contain many hydrogens and the incoherent atomic scattering cross section of hydrogen is much larger than the incoherent and coherent atomic scattering cross sections of other atoms as well as the coherent one of hydrogen[7].

A part of analysis of the observed dynamic scattering laws was carried out by curve fitting with model functions using the computer codes QUESA40[5] and QUESA80[5].

3. Dynamics in the Glassy State

Major differences of dynamics between amorphous and crystalline materials can be recognized in the low energy range below ca. 10 meV at low temperatures enough below the glass transition where any relaxation processes cannot be observed in amorphous materials. This is macroscopically manifested as anomalous thermal properties of amorphous materials such as heat capacity[8]. The heat capacity C(T) of amorphous materials exceeds that expected for crystalline materials (Debye solids) in two low temperature ranges. One is the range below 1K, where C(T) is proportional to T, and the other is the range of 2–20K. These excess heat capacities are due to excess excitations of the amorphous materials in the corresponding energy ranges. The excess heat capacity below 1K is well explained by a tunneling model in a double well potential. However, the nature of the tunneling motion

is still unknown. Less understood is the excess heat capacity in the temperature range 2–20K, which corresponds to the excess excitations in the energy range 1–5 meV. Recently, inelastic neutron scattering studies have been extensively made on this excitation (*low energy excitation*), but there remain many unsolved problems.

In this section, we present the inelastic neutron scattering studies on the *low energy excitations* in amorphous polymers and discuss the results in terms of an asymmetric double well potential.

3.1 Low Energy Excitation in Amorphous and Crystalline Phases

In order to clarify the differences between the low energy excitations of amorphous and crystalline phases, inelastic neutron scattering measurements have been made on polyethylenes as a function of degree of crystallinity at 10K[9]. The dynamic scattering laws $S(Q,\omega)$ of the crystalline and amorphous phases of PE are shown in Fig. 1(a). In the spectrum of the amorphous phase of PE, a broad peak is observed at about 3 meV. This broad peak is absent in the spectrum of the crystalline phase. We may then directly conclude that the *low energy excitation* at around 3 meV is characteristic of the amorphous phase.

The density of states $G(\omega)$ is plotted in the form $G(\omega)/\omega^2$ versus ω for the amorphous and crystalline phases in Fig. 1(b). The figure shows that $G(\omega)$ of the crystalline phase is *approximately* proportional to ω^2. This means that the excitations in the crystalline phase can be described by the Debye theory in the examined energy range. For the amorphous phase, $G(\omega)/\omega^2$ shows a peak at about 2.5 meV and the value of $G(\omega)$ is much larger than that of the crystalline phase. In the low energy range below 1 meV, $G(\omega)$ of the amorphous phase seems to vary in proportion to ω^2, suggesting that $G(\omega)$ of the amorphous phase is dominated by the Debye mode (sound wave) below 1 meV. This was confirmed from calculation of the sound velocity in both the amorphous and crystalline phases[9].

The heat capacity C(T) was calculated from the density of states $G(\omega)$ in Fig. 1(b) for the amorphous and crystalline phases in the temperature range of 2 to 15K and the results are plotted as $C(T)/T^3$ in Fig. 1(c). The agreement between the temperature dependence of the calculated and observed $C(T)/T^3$ is fairly good. It is confirmed that the *low energy excitation* at around 2–3 meV of the amorphous phase is the origin of the excess heat capacity of the amorphous phase.

3.2 Universality of Low Energy Excitation

Thermal anomaly at low temperatures is observed for many amorphous materials, suggesting that the *low energy excitation* should be the common characteristic of amorphous materials. In order to confirm this, we carried out inelastic neutron scattering measurements on various amorphous polymers as well as inorganic glasses[10]. Organic polymers used for the scattering experiments are polyisobutylene (PIB), cis-1,4-polybutadiene (PB), cross-linked cis-1,4-polybutadiene (cl-PB), trans-1,4-polychloroprene (PCP), atactic polystyrene (PS), highly crystalline polyethylene (h-PE) with degree of crystallinity 0.96, semi-crystalline polyethylene (s-PE) with degree of crystallinity 0.46 and epoxy resin (EXPO) cured with polyamide amine. Three inorganic glasses of germanium (GeO_2), boric oxide (B_2O_3) and amorphous selenium (Se) are also used.

In Fig. 2, observed dynamic scattering laws $S(Q,\omega)$ measured with LAM-40 are shown

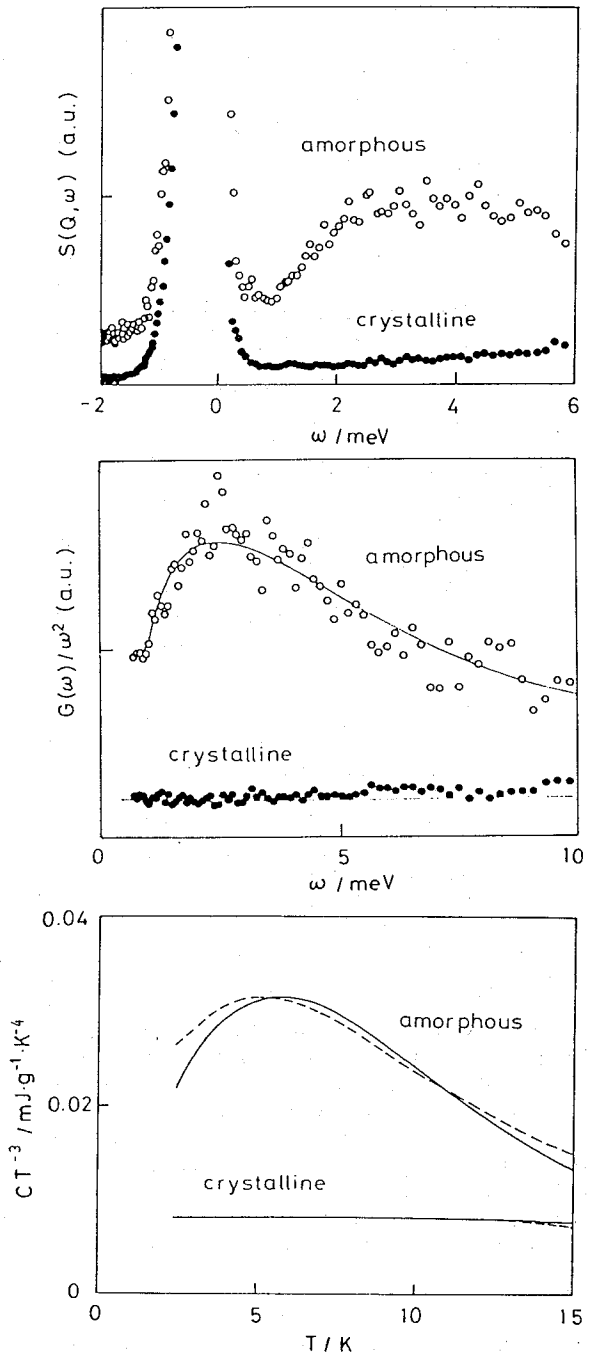

Fig. 1. (a) Dynamic scattering laws $S(Q,\omega)$ for amorphous and crystalline phases of PE at 10K. (b) Density of states $G(\omega)$ for amorphous and crystalline phases of PE plotted as $G(\omega)/\omega^2$ against ω. Solid lines are fitting curves. (c) Heat capacity C(T) for amorphous and crystalline phases of PE. Solid lines were calculated from the fitting curves of $G(\omega)$ in (b) and dashed lines are from experimental data [J.E. Tucker and W. Reese, *J. Chem. Phys.*, **46**, 1388 (1967).].

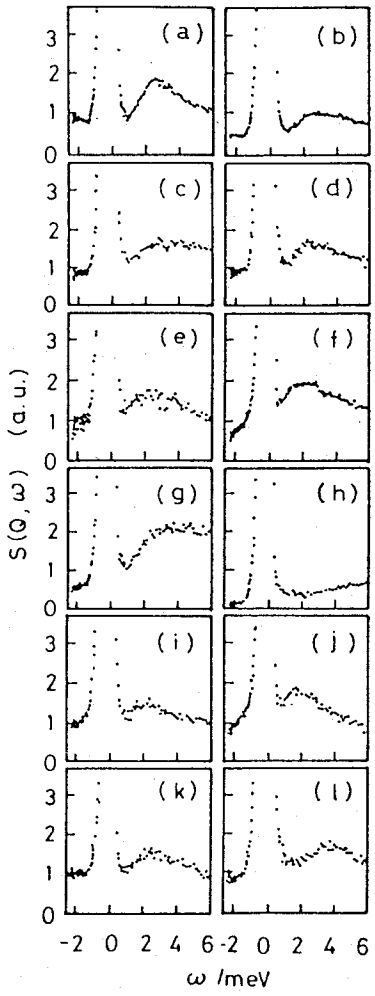

Fig. 2. Dynamic scattering laws $S(Q,\omega)$ for various amorphous polymers. (a) polyisoprene (PIB) at 50K; (b) PIB at 10K; (c) cis-1,4-polybutadiene (PB) at 50K; (d) cross-linked PB at 50K; (e) trans-1,4-polychloroprene (PCP) at 50K; (f) atactic polystyrene (PS) at 10K; (g) semicrystalline polyethylene (s-PE) with degree of crystallinity of 0.46 at 10K; (h) highly crystalline polyethylene (h-PE) with degree of crystallinity of 0.96 at 10K; (i) epoxy resin (EXPO) at 50K; (j) amorphous selenium (a-Se) at 150K; (g) germanium (GeO_2) glass at 295K; (l) boric oxide (B_2O_3) glass at 295K. Spectra of (a)-(i) are obtained by summing up the seven spectra at scattering angles at 8°, 24°, 40°, 56°, 72°, 88°, and 104°. Spectra of (j)-(l) are at $Q=2.07$ Å^{-1}.

for eight organic polymers and three inorganic glasses. All the samples except highly crystalline polyethylene (h-PE) show a broad excitation peak in the energy range of 1.5–4.0 meV. These data strongly demonstrate that the *low energy excitation* is a universal property for amorphous materials.

The *low energy excitation* appears irrespective of differences in chemical structures of amorphous materials. However, the details in the energy, shape and intensity of the peak

depend on the chemical structure and temperature. Studies on partially deuterated PS[11] revealed that the *low energy excitation* peak of the main chain (methylene chain) appears at 1.5 meV, which is 0.7 meV lower than that of the side chain (phenyl group). This energy shift has been assigned to the larger effective mass of the main chain.

3.3 Origin of Low Energy Excitation[10]

Some models have been proposed to explain the *low energy excitations* in amorphous materials. Recent fashionable explanation is by "fracton"[12], which is an excitation in fractal networks. This idea was successfully applied to the density of states of cross-linked expoxy resin[13] but failed to explain the dynamic structure factors of vitreous silica and amorphous germanium. Buchenau assigned the origin of these excess *low energy excitations* to a coupled rotation of five SiO_4[14] and a bond bending mode[15], respectively, by analyzing the coherent dynamic structure factor. Buchenau have also shown that these motions have a common origin, the so-called "asymmetric double-well potential"[16]. This idea is very attractive because the universality of the *low energy excitation* should require a common microscopic picture for all the amorphous materials. In this sense, we believed that the "asymmetric double-well potential" is valuable to examine as a common origin of the *low energy excitation*.

We begin with the analysis of Q dependence of the inelastic scattering intensity of the *low energy excitation* to obtain the spatial information of the motion. According to a classical picture of the asymmetric double-well potential, the dynamic scattering law $S(Q,\omega)$ is given by

$$S(Q,\omega)=S_{el}(Q,\omega)+S_{in}(Q,\omega)$$

$$= \exp(-\langle u^2\rangle Q^2)\{1-2\,f\,p_1\,p_2\,[1-j_0(Qd)]\}\,\delta(\omega) + \exp(-\langle u^2\rangle Q^2)\,2\,f\,p_1\,p_2\,[1-j_0(Qd)]\,F(\omega) \qquad (1)$$

where $\delta(\omega)$ is a δ-function, $F(\omega)$ is a frequency distribution of the motion, f is the fraction of hydrogens participating in the motion, d is the distance between the two sites, j_0 is the *zero-th* order spherical Bessel function and $\langle u^2\rangle$ is the mean square amplitude of oscillatory motions in the well. p_1 and p_2 are the probabilities to find a scattering particle on sites 1 and 2, respectively, and related to the energy asymmetry through

$$p_1/p_2=\exp(-\Delta H/kT) \qquad (2)$$

where ΔH is the energy difference between the two sites.

The Q dependence of the inelastic scattering intensity $I_{LEE}(Q)$ of the *low energy excitation* of PIB is plotted against Q^2 in Fig. 3. $I_{LEE}(Q)$ is not proportional to Q^2, suggesting that the *low energy excitation* is not harmonic. The solid line in Fig. 3 indicates a fitted theoretical function $1-j_0(Qd)$ in the inelastic part of eq.(1) where d was taken to be 1.17 Å. The agreement is very good, showing that the two-site motion can describe the Q dependence. The value of d corresponds to an average distance of the displacement of hydrogens. In the case of PIB, hydrogens cannot move individually but probably as an atomic group in-

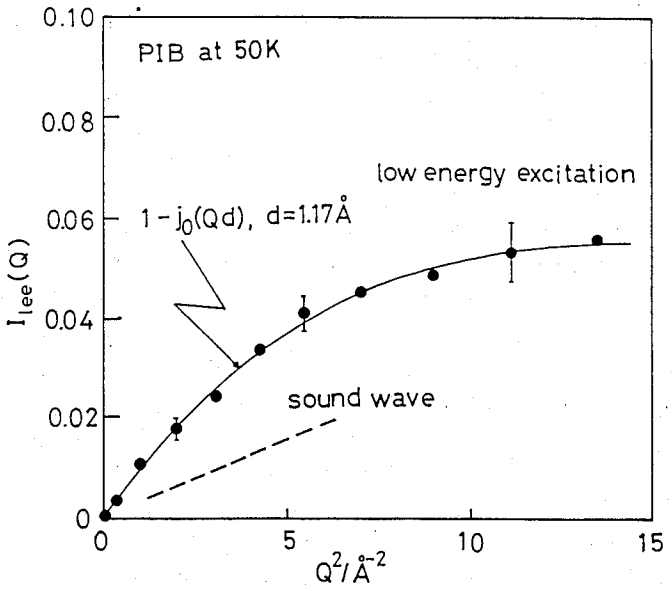

Fig. 3. Inelastic scattering intensity of the *low energy excitation* as a function of Q for PIB at 50K. The intensity $I_{LEE}(Q)$ is obtained by integrating in the ω-range $0<\omega<6$ meV after correcting the Debye-Waller factor $\exp(-\langle u^2\rangle Q^2)$ and subtracting the sound wave contribution and elastic scattering. Intensity from the sound wave is indicated by a dashed line for comparison. The solid line represents the fitting result with function $1\text{-}j_0(Qd)$ with $d=1.17$ Å.

cluding carbons. Therefore, it is noted that the distance d does not directly correspond to the displacement of the centre of an atomic group (a mobile group) as far as the *low energy excitation* mode is concerned.

In the next step, we study eigen values of the asymmetric double well potential. For this purpose, we must discard the classical picture. Our starting point is the Schrödinger equation.

$$H\phi_n=E_n\phi_n \tag{3}$$

where $H=K+V$ and H, E_n, ϕ_n, K and V are the Hamiltonian of the asymmetric double well potential, the eigen value for the n-th state, the wave function for the n-th state, the kinetic energy and the potential energy, respectively. We have employed the following function to represent the asymmetric double well potential:

$$V(r)=a_1 r+a_2 r^2+b\exp(-c r^2). \tag{4}$$

In our measurements, the observed excitation energy ω_0 is given by

$$\omega_0=\Delta E=E_1-E_0 \tag{5}$$

where E_0 and E_1 are the eigen values for the ground and first excited states. The inelastic scattering intensity $I_{in}(Q)$ of a powder sample is proportional to the transition probability P(Q) from the initial state to the final state, which is given by

$$P(Q)=\langle | \int \phi_1(\mathbf{r}) \exp(i\,\mathbf{Qr})\ \phi_0(\mathbf{r})\ d\mathbf{r} |^2 \rangle . \tag{6}$$

Substituting eq.(4) into eq.(3), we numerically solved the Schrödinger equation by surveying the potential parameters and the mass of mobile group and calculated the excitation energy ω_0 and the transition probability P(Q). It was found that appropriate sets of the potential parameters can reproduce the experimental values. An example of such asymmetric double well potential and the corresponding wave function are shown in Fig. 4. The ranges of the potential parameters which reproduce the experimental observations are summarized in Table I and the corresponding range of the barrier height V_0, the energy

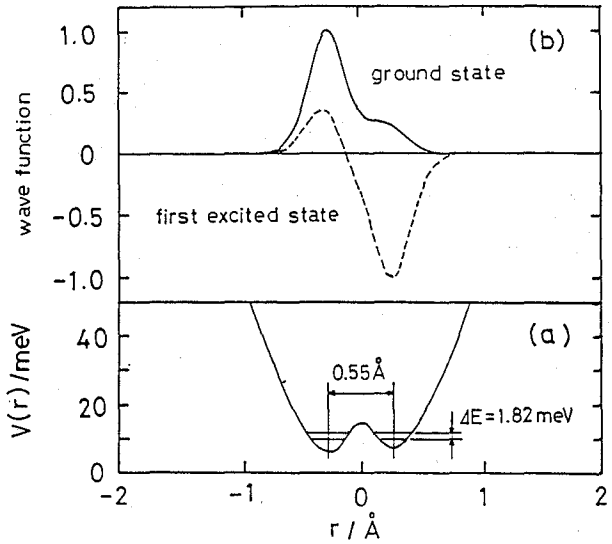

Fig. 4. (a) A typical asymmetric double-well potential $V(r)=a_1r+a_2r^2+b\exp(-cr^2)$; $a_1=3$ meV, $a_2=60$ meV Å^{-2}, $b=15$ meV, $c=24$ Å^{-2}. (b) Wave function of the ground state (solid line) and of the first excited state (dashed line). Mass of a mobile group m is 20 amu. Parameters for the potential are the same as in (a).

Table I. Ranges of parameters for the asymmetric double-well potential:
$V(r)=a_1r+a_2r^2+b\exp(-cr^2)$.

a_1 (meV Å^{-1})	a_2 (meV Å^{-2})	b (meV)	c (Å^{-2})	m (amu)	V_0 (meV)[a]	ΔH (meV)[b]	d_{min} (Å)
2–8	~60	10–25	~24	12–40	4–16	1–4	0.5–0.62

[a] $V_0=V(r_{max})-[V(r_{min,1})+V(r_{min,2})]/2$.
[b] $\Delta H=V(r_{min,2})-V(r_{min,1})$.

asymmetry ΔH and the distance between the two minima d_{min} are also listed in Table I.

The fraction of the hydrogens taking part in the *low energy excitation* mode can be calculated from eq.(1) using the value of the energy asymmetry ΔH and the distance between the two minima d. In the case of PIB, ΔH ranges from 1 to 4 meV. This corresponds to the range of $p_1p_2=0.247-0.203$ at 50K. The distance between the two minima d has been evaluated to be 1.17 Å, so that the range of the fraction f is estimated to be 0.083 to 0.10 at 50K. In the amorphous PIB, about 9% of the hydrogens take part in the asymmetric double well potential system.

The next problem to be answered is the temperature dependence of the inelastic intensity. The density of states $G(\omega)$ of PIB at 10K and 50K are shown in Fig. 5, where $G(\omega)/\omega^2$ is plotted against ω. Both of the $G(\omega)$'s are essentially identical. This means that the temperature dependence of the inelastic scattering intensity can be reduced by the Bose factor. This result is usually interpreted by assuming that the *low energy excitation* is harmonic. On the other hand, it is predicted from the Q dependence of the inelastic intensity that the *low energy excitation* is not harmonic; the inelastic intensity is not proportional to Q^2 (see Fig. 3). As the asymmetric double well potential is clearly inharmonic, a problem that we should answer is why the temperature dependence can be described by the Bose factor. A possible answer is given by a concept of "phonon-assisted tunneling". In amorphous polymers, there exist asymmetric double-well potential sites (ca. 9% in PIB) and also propagating phonons (sound wave). The asymmetric double-well potentials interact with the propagating phonons through deformation of the double well potential by the elastic wave. When the phonon energy is near or equal to the energy difference between the ground and first excited states, it will be resonantly absorbed and then reemitted

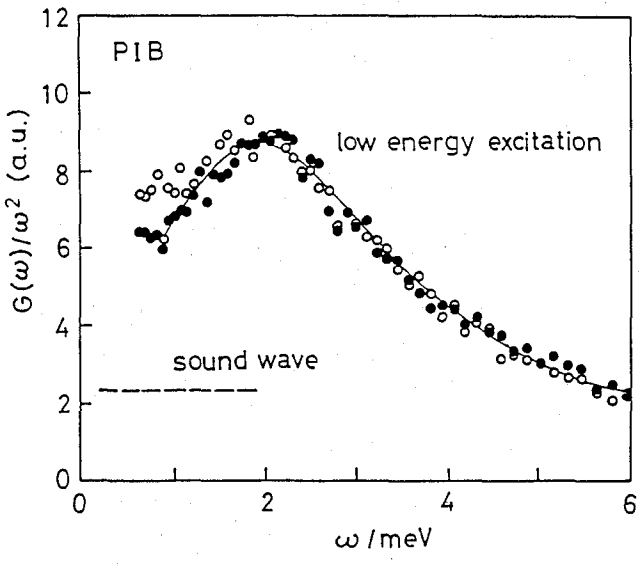

Fig. 5. Density of states $G(\omega)$ for PIB plotted as $G(\omega)/\omega^2$ against ω. (●) from the data at 50K; (○) from the data at 10K. The dashed line indicates the contribution of the sound wave. The solid line is the result of fitting to $G(\omega)/\omega^2$ at 50K.

incoherently. Even though the mobile group does not have sufficient energy to surmount the barrier because of very low temperature, it can move from one minimum to the other through the phonon-assisted tunneling process. If the interactions are so frequent, the population in the asymmetric double well potential is governed by that of the propagating phonons, i.e., the Bose factor. This picture seems to well explain our results.

4. Dynamics near the Glass Transition

The glass transition is a universal phenomenon for all glass forming materials[17]. In the cases of polymer systems, even crystalline polymers include some amounts of amorphous regions because polymers cannot be fully crystallized due to the topological restrictions and it is well known that some properties of polymers such as mechanical properties depends on the nature of the amorphous regions[18]. Therefore, many investigations have been theoretically and experimentally performed on the glass transition though most of them have been engaged in phenomenological models for the macroscopic nature such as mechanical and thermal properties. Recently, a microscopic theory, the so-called mode coupling theory[19], has been developed based on an equation for the density autocorrelation function containing a nonlinear memory function and gives some detailed pictures and predictions for the dynamical process near the glass transition, e.g., ergodic-nonergodic dynamical transition occurs at a critical temperature T_c which exists above the calorimetric glass transition temperature T_g. Stimulated by the theory, a lot of experimental works[20] were carried out on inorganic and organic glass forming materials as well as polymers using inelastic neutron scattering, light scattering and dielectric relaxation techniques.

In this work, we performed quasielastic neutron scattering measurements on cis-1,4-polybutadiene in a wide temperature range covering T_g(=170K) and found that two modes of motion appear near T_g in the energy ranges of ca. 1 meV and 10~30 meV, respectively. The fast mode arises ca. 50K below T_g, which corresponds to the so-called Vogel temperature T_0. On the other hand, the slow mode appears just above T_g. In this section the natures of the two modes are discussed from viewpoint of glass transition.

4.1 The Fast Mode (β-process)[21]

Dynamic scattering laws $S(Q,\omega)$ of cis-1,4-polybutadiene (PB) measured with LAM-40 are shown in Fig. 6 as a function of temperature. The spectra enough below T_g show a broad *low energy excitation* peak at ω=2~3 meV. The dashed lines in Fig. 6 show the values expected from the Bose factor, which were calculated based on the 50K data. The spectrum at 100K agrees very well with the expected value, confirming that the intensity of the *low energy excitation* of PB can be also normalized by the Bose factor. On the other hand, the spectrum at 170K (=T_g) shows an additional quasielastic scattering intensity below ca. 4 meV and the excess intensity gradually increases with temperature as can be seen in the spectra at higher temperatures. The excess quasielastic intensity must correspond to a new relaxation process. The excess intensity at ω=1 meV is plotted against temperature in Fig. 7. The solid line in Fig. 7 is the result of the fit with $(T-T_f)^\gamma$ for γ=1.6, where T_f is a critical temperature at which the excess quasielastic intensity begins to arise, and we found T_f=119K. This temperature is ca. 50K below T_g and corresponds to the so-called

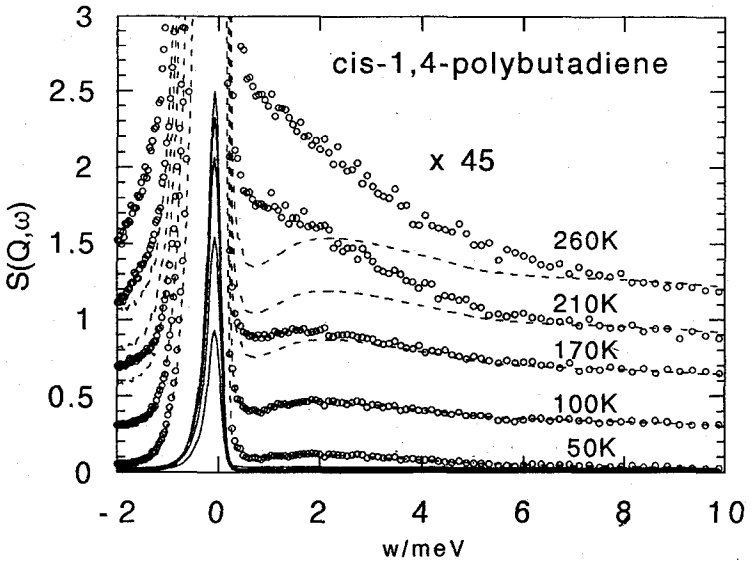

Fig. 6. Dynamic scattering laws $S(Q,\omega)$ of cis-1,4-polybutadiene (PB) measured by LAM-40 below and above the glass transition temperature T_g (=170K). The spectra were obtained by summing up 6 spectra at scattering angle 24°, 40°, 56°, 72°, 88° and 104° and the average Q value is 1.54 $Å^{-1}$. The spectra are expanded by a factor 45 and shifted by 0.2 for each. Dashed lines are the values expected from the Bose factor, which were calculated based on the spectrum at 50K.

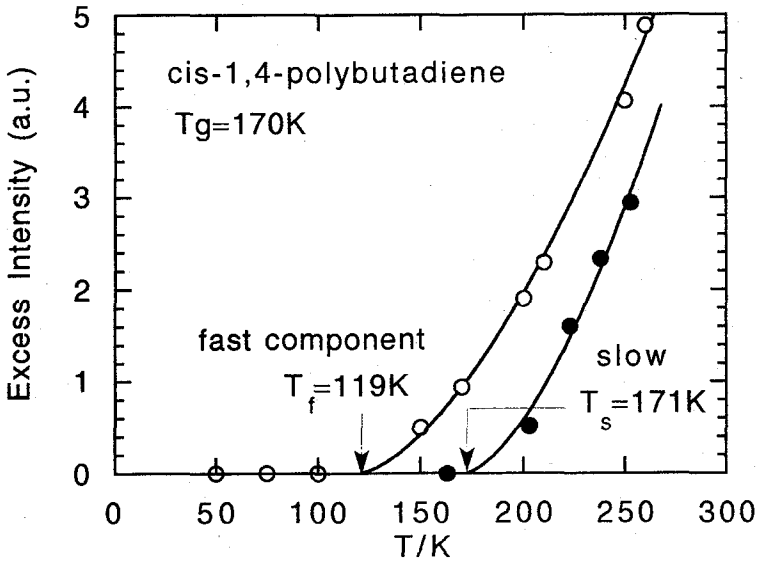

Fig. 7. Temperature dependence of the scattering intensities for the faster and slower quasielastic components. Solid lines are the results of the fit with $(T-T_i)^\gamma$ (i=f and s, γ=1.6). The critical temperatures T_f and T_s are 119K and 171K for the faster and slower components, respectively.

Vogel temperature T_0, which is usually observed ca. 50K below T_g for most of all amorphous polymers[18]. It is considered that the temperature T_f ($=T_0$) is the lowest temperature at which the fastest relaxation process (β-process) can be observed.

The spectra for only the excess scattering intensity were obtained by subtracting the calculated values using the 50K data and the Bose factor from the observed $S(Q,\omega)$. The difference spectra were fitted with a single Lorentzian convoluted with the resolution function of LAM-40. The estimated half-width at half-maximum (HWHM) Γ_f is plotted as a function of temperature in Fig. 8. The Γ_f is almost independent of both Q and temperature, suggesting that the motion observed here is very localized. A problem that we have to consider is what the localized motion is. As will be shown in the next section, Γ_f in the melt slightly depends on temperature, giving the activation energy of ca. 0.5 kcal/mol (see Fig. 8) and we have assigned this motion to the damped vibrational motion in the C-C torsional potential. The activation energy for the localized motion (ca. 0.5 kcal/mol) is very low compared with the barrier height for the C-C torsional potential (2~3 kcal/mol). This very low barrier may be produced by distortion of the torsional potential due to strains of surrounding polymer chains. Alternatively, in the study of the *low energy excitation* of amorphous polymers at temperatures enough below the T_g, we found that the energy barrier height of the asymmetric double well potential in the glassy state is in the range of 0.1 to 0.4 kcal/mol. This height is very close to the activation energy observed in the melt.

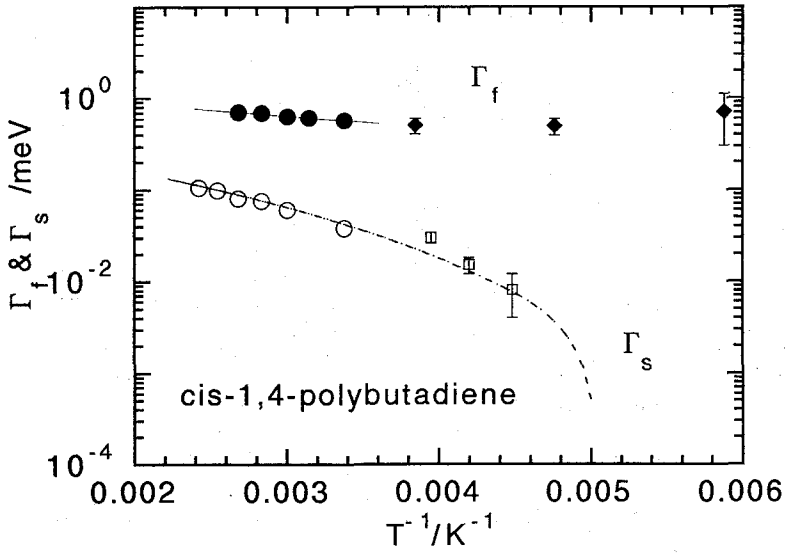

Fig. 8. Temperature dependences of HWHM of the fast and slow quasielastic components Γ_f and Γ_s, which were evaluated from LAM-40 and LAM-80 data, respectively. In the molten state (T>Tm=2°C), temperature dependences of Γ_f (●) and Γ_s (○) are described by the Arrhenius form and the corresponding activation energies are ca. 0.5 kcal/mol and 2.5 kcal/mol, respectively. In the whole temperature range including the supercooled state, temperature dependence of Γ_s is described by the WLF form. Dashed line is the result of the WLF fit for Γ_s. $C_1=8.43$, $C_2=51.4$, $\Gamma_0=1.05\times10^{-4}$ [see eq.(7)]. Q values are (○); 1.23 $Å^{-1}$, (●); 1.21 $Å^{-1}$. (●); 2.07 $Å^{-1}$, (◆); 1.54 $Å^{-1}$. Note that Γ_f is almost independent of Q.

Therefore, it is considered that the asymmetric double well potential in the glassy state is a frozen state of the distorted potential observed in the melt. At a very low temperature, atomic groups (parts of polymer chain) trapped in one site of the asymmetric double well potential cannot move to another site passing over the barrier even if the barrier height is very low. As temperature increases, the atomic groups are gradually thermally activated and begin to surmount the barrier (ca. 0.1~0.5 kcal/mol) at a critical temperature T_f (= T_0), which is probably observed in this study. Even above T_f, the atomic groups are still trapped within the C-C torsional potential well. In this sense, the localized motion can be called as a "cage motion". As temperature further increases, the atomic groups would be more activated enough to pass over the barrier for the C-C torsional potential (2~3 kcal/mol), leading to the structural relaxation or the α-relaxation. This process is observed using the high resolution machine LAM-80 as will be shown below.

4.2 The Slow Mode (α-process)[21,22]

The high resolution spectrometer LAM-80 can access the energy range of 0.01 to 0.3 meV which is rather smaller than that of LAM-40, so that we can observe slower motions. Dynamic scattering laws $S(Q,\omega)$ observed with LAM-80 are shown as a function of temperature in Fig. 9. We can observe the onset of a new quasielastic scattering component in the energy range below ca. 0.1 meV near T_g. The intensity of the slow (narrow) quasielastic component in the ω-range of 0.02 to 0.2 meV is shown in Fig. 7 as a function of temper-

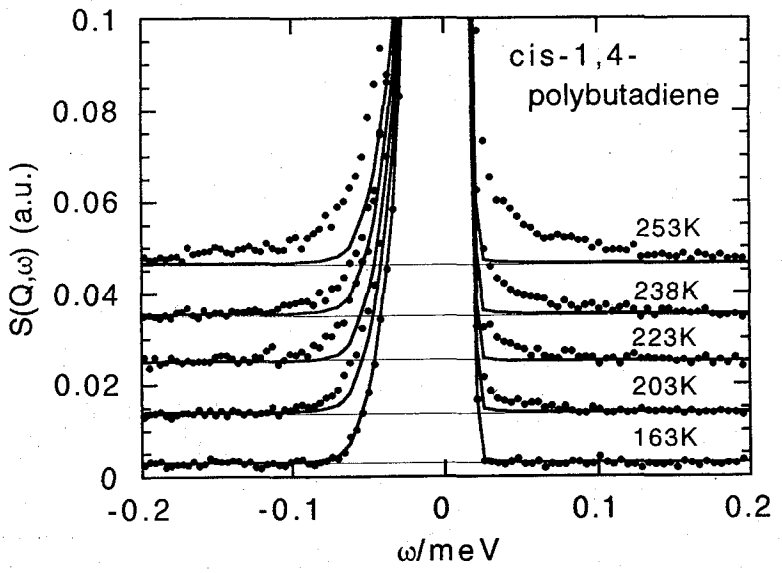

Fig. 9. Dynamic scattering laws $S(Q,\omega)$ of cis-1,4-polybutadiene (PB) measured by LAM-80 below and above the glass transition temperature T_g (=170K). The spectra were obtained by summing up 3 spectra at scattering angles 35, 80 and 135° and the average Q value is 1.21 $Å^{-1}$. Flat thin solid lines are the contributions of the fast quasielastic component observed LAM-40. The thick solid lines are the resolution function of LAM-80. Note that the spectrum at 163K (below T_g) is identical with the resolution function.

ature. The solid line in Fig. 7 is the result of the fit with $(T-T_s)^{\gamma}$ for $\gamma=1.6$, giving a critical temperature $T_s=171K$ at which the slow component begins to arise. The temperature T_s is very close to the glass transition temperature T_g.

As a first approximation we fitted the observed $S(Q,\omega)$ with sum of a δ-function and a single Lorentzian convoluted with the resolution function of LAM-80. The HWHM Γ_s of the Lorentzian is plotted against 1/T also in Fig. 8. The temperature dependence of Γ_s in the molten state can be described by the Arrhenius form and the activation energy evaluated in the molten state is in the range of 2~3 kcal/mol[26], suggesting that the slow mode can be related to the local conformational transition of PB. The conformational transition should make the structural relaxation. In a sense of glass transition dynamics, we can call the slow mode as the α-relaxation process. On the other hand, Γ_s gradually deviates from the Arrhenius form with decreasing temperature. The temperature dependence were fitted with the Williams-Landel-Ferry (WLF) equation in the whole temperature range.

$$\log(\Gamma_s)=\log(\Gamma_0)+C_1(T-T_g)/(C_2+T-T_g) \qquad (7)$$

The result is shown in Fig. 8 by a dashed line. The agreement is rather good. This fact also supports that the slow mode is related to the structural relaxation or the α-relaxation. The WLF behaviour should be due to some kind of correlated motion near the T_g. It is noted that the parameter C_2 in eq.(7) was estimated to be 51.9K in the fit. The corresponding Vogel temperature T_0 is calculated from T_g-C_2 to be 118.1K. This value agrees excellently with the estimated value T_f (=119K) from the fast quasielastic component.

5. Dynamics in the Molten State

In polymer chains, conformational transitions between rotational isomeric states are fundamental to the understanding of many of the rapid relaxation processes. Crankshaft-like motions such as Schatzki crankshaft[23] or three bond motion[24] were considered to be the most reasonable explanation of the local motions. However, recent important progress in this field has provided an argument against the crankshaft-like motions. Helfand and coworkers[25] have made computer simulations by employing a realistic polymer chain involving bond rotation, bond angle bending and bond length stretching and found that isolated transitions as well as cooperative transitions occur.

Our attention is focused on the mechanism of the local conformational transition in polymer chains in this section. As shown in computer simulations, the conformational transitions are assisted by distortions in a polymer chain through vibrational motions, especially bond rotations or torsional vibrations. We are also interested in the vibrational motions, which are probably damped due to thermal agitations or high friction in both solution and melt.

In this section, we present the experimental results of quasielastic neutron scattering on cis-1,4-polybutadiene in the melt. In the time range of 10^{-13} to 10^{-10} s, there exist two modes of motion. These correspond to the fast and slow modes appearing at ca. 50K below T_g and just above T_g, respectively, which were revealed in the previous section. The fast and slow modes can be assigned to the damped torsional vibration (bond rotation) and

the local conformational transitions, respectively. The results are analyzed in terms of a jump diffusion model with the damped vibrational motions.

5.1 Damped Vibrational Motion in C-C Torsional Potential[26]

The observed dynamic scattering laws $S(Q,\omega)$ of PB in the melt observed with LAM-40 at $Q=1.76$ Å^{-1} are shown in Fig. 10 as a function of temperature. All the spectra were well fitted with sum of a δ-function and two Lorentzians as shown by solid lines in the figure. Judging from the low temperature data presented in the previous section, the broad and narrow quasielastic components should correspond to the damped *low energy excitation* mode and the fast mode (β-process) appearing at ca. 50K below T_g, respectively. The HWHM's of both components show the same temperature and Q dependences. This indicates that the two components are strongly coupled in the melt. The very weak temperature dependences give an activation energy of E_a=ca. 0.5 kcal/mol (Fig. 8). This value of E_a is too small for local conformational transitions. The HWHM's of the two components are also independent of Q, suggesting that the fast mode is very localized.

There are two possibilities for this restricted motion: (1) damped vibrational motion and (2) diffusive motion in a finite volume (a cage). However, it is difficult to distinguish these two possibilities from the observed scattering spectra because both motions are very similar to each other under the condition of strong damping. In the present state, we assigned the fast mode to a damped torsional vibrational motion because it is the softest

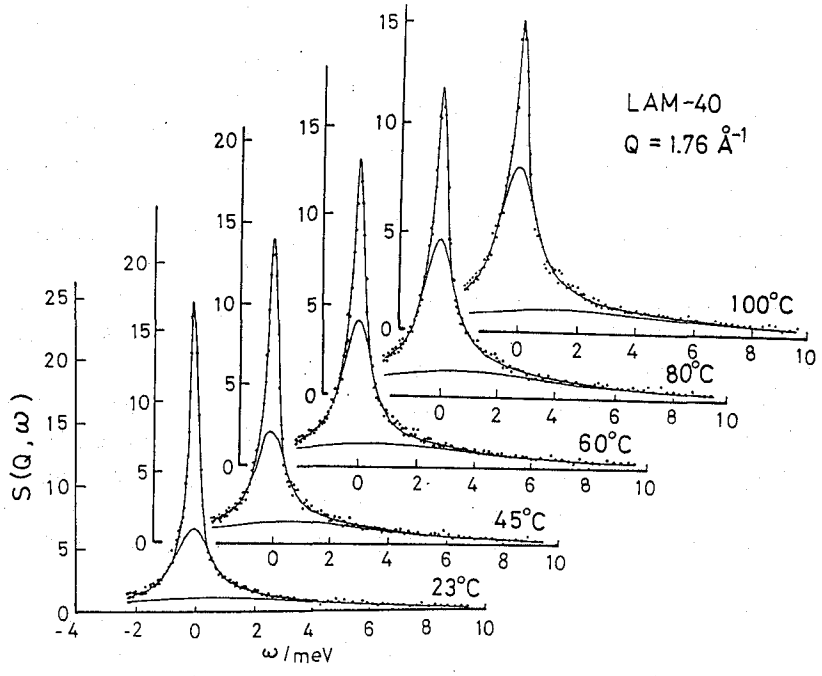

Fig. 10. Dynamic scattering laws $S(Q,\omega)$ of cis-1,4-polybutadiene (PB) in the melt measured by LAM-40 at $Q=1.76$ Å^{-1} as a function of temperature from 23°C to 100°C. Solid lines represent the fitting results including elastic and two quasielastic components.

mode and the amplitude of hydrogen atom displacement is larger than those of other modes.

The potential shape for the torsional vibration can be described by a quadratic form in the crystalline states. However, it is natural to consider that the shape in the molten state is distorted by strain due to the local conformational transition and/or surrounding polymer chains. The activation energy (ca. 0.5 kcal/mol) should reflect the low barrier caused by the distortion.

5.2 Local Conformational Transition[26]

The slow mode in the melt, which appears just above T_g, was studied by the high resolution spectrometer LAM-80. The observed dynamic scattering laws $S(Q,\omega)$ of PB at $Q=1.23$ Å^{-1} are shown in Fig. 11 as a function of temperature. The narrow quasielastic

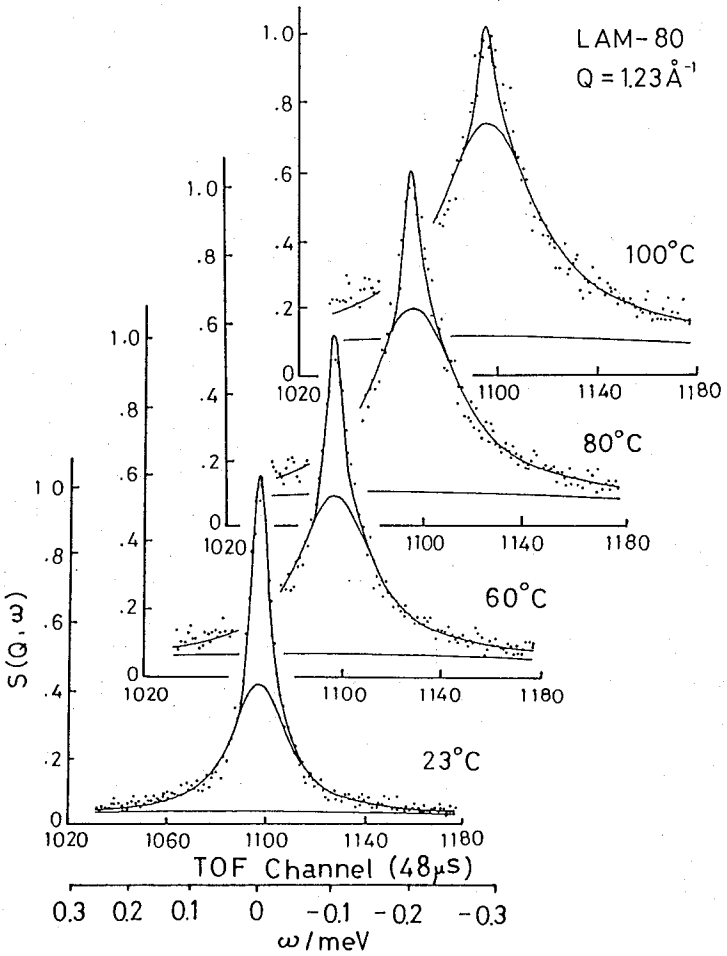

Fig. 11. Dynamic scattering laws $S(Q,\omega)$ of cis-1,4-polybutadiene (PB) in the melt from 23°C to 100°C measured by LAM-80. Solid lines represent the fitting results including elastic and quasielastic scattering components. The almost flat lines represent the very broad quasielastic components observed by LAM-40.

scattering component (the slow mode) can be clearly observed in the spectra. This component can be well fitted with a single Lorentzian as shown by solid lines in the figure. The Arrhenius plot of HWHM of the slow component in the melt gives an activation energy ca. 2.5 kcal/mol (see Fig. 8). This value corresponds nearly to the height of one energy barrier separating rotational isomeric states. It means that the slow mode can be related to the local conformational transitions.

For description of the local conformational transition, we adopted a jump diffusion model with the damped vibrational motions by taking into account the results of the computer simulation by Helfand[25]. The schematic sketch of the jump diffusion model is shown in Fig. 12. Thus, (1) in this model, conformational transitions should be accompanied with

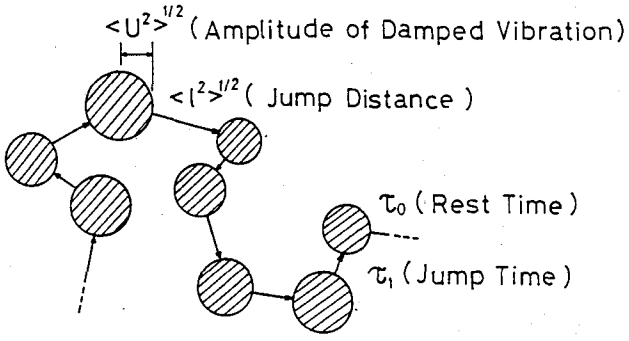

Fig. 12. Schematic sketch of the jump diffusion model with damped vibrational motions. It is assumed that $\tau_0 \ll \tau_1$ in the present analysis so that τ_0^{-1} corresponds to the local conformational transition rate.

the damped vibrational motions. These motions assist distortions of degree of freedom in the neighbourhood of the conformation-transforming bond and keep the transition localized. The spatial scale of the damped vibrational motion has been evaluated as $\langle u^2 \rangle$ obtained in LAM-40 measurements. (2) We define the average rest time τ_0 for a conformation (lifetime of conformation) and the average jump time τ_1 between the different conformations. Assuming $\tau_1 \ll \tau_0$, the rate of the conformational transition is given by τ_0^{-1}. (3) The mean-square jump distance between different conformations is defined as $\langle l^2 \rangle$. (4) The transitions occur successively in the neighbourhood of the previous transition. This succession leads to a physical picture of jump diffusion of the transition states. (5) We assume that all the motions are isotropic. The dynamic scattering law of this model $S_{jd}(Q,\omega)$ under the condition $\tau_0 \gg \tau_1$ is given by[27]

$$S_{jd}(Q,\omega)=(1/\pi)\ \Gamma_{jd}\ \exp(-\langle u^2 \rangle\ Q^2)/(\omega^2+\Gamma_{jd}^2) \tag{8}$$

$$\Gamma_{jd}=[DQ^2+(1-\exp(-\langle u^2 \rangle\ Q^2))/\tau_0]/[1+DQ^2\ \tau_0] \tag{9}$$

where D is the diffusion coefficient of transition site, given by $\langle l^2 \rangle/6\tau_0$. $S_{jd}(Q,\omega)$ can be represented by a Lorentzian with HWHM Γ_{jd}. This agrees with our observation.

In order to evaluate the parameters τ_0 and $\langle l^2 \rangle$ in the jump diffusion model, the Q dependence of HWHM of the slow mode is fitted with the theoretical function (eq.(9)). In Fig. 13 the Q dependence of HWHM of the slow mode is shown for 23, 60, 80, 100, 120 and 140°C. Solid lines in the figure are the results of the fit. The agreement is very good and it is confirmed that the jump diffusion model is appropriate to describe the local conformational transitions. The values of τ_0 and $\langle l^2 \rangle$ are summarized in Table II where the

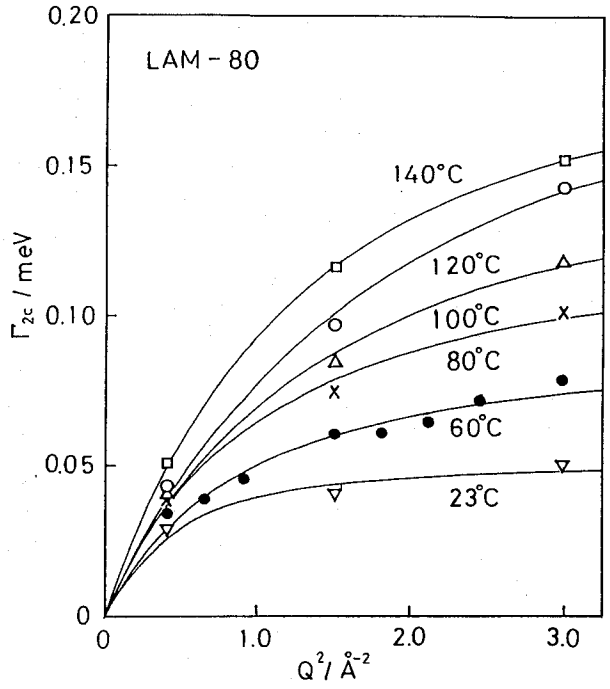

Fig. 13. Q^2 dependence of half-width at half-maximum (HWHM) of the slow quasielastic component revealed by LAM-80. (▽) 23°C; (●) 60°C; (×) 80°C; (△) 100°C; (○) 120°C; (□) 140°C. Solid lines represent the best fit with eq.(8).

Table II. Parameters of the Jump Diffusion Model for the Local Conformational Transitions Determined from LAM-40 and LAM-80 Data

T/°C	$\langle U^2 \rangle$/ Å^2	$\langle l^2 \rangle^{1/2}$/ Å[a]	τ_0/ps[b]	$D/10^2$Å^2 ps^{-1} [c]	τ_K/ps[d]
23	0.44	(3.71)	81.0	(4.5)	102
45	0.49				72.6
60	0.51	2.31	48.6	1.8	59.1
80	0.55	2.12	35.6	2.1	46.0
100	0.58	1.76	28.9	1.8	36.8
120	0.62	1.43	22.4	1.5	30.2
140	0.66	1.85	21.2	2.7	25.3

[a] Value of $\langle l^2 \rangle^{1/2}$ calculated from molecular structure is 2.03 Å. [b] Activation energy of τ_0 (E^*) is 2.9 kcal/mol. [c] Calculated from $D = \langle l^2 \rangle / 6\tau_0$. [d] Calculated from Kramers' rate theory.

diffusion coefficient D ($=\langle l^2\rangle/6\tau_0$) are also listed. The value of $\langle l^2\rangle$ are almost independent of temperature, indicating that the mechanism of the local conformational transition does not change in the observed temperature range. The activation energy of τ_0 is estimated to be 2.9 kcal/mol from the Arrhenius plot of τ_0. This value is almost the same as the height of one barrier separating rotational isomeric states.

4.3 Comparison with Rate Theory

In this section, we will compare the rest time τ_0 with Kramers' rate theory[28]. According to the rate theory, the conformational transition rate k_K is given by

$$k_K=\{(\gamma_A\gamma_B)^{1/2}/(2\pi\xi)\}\ [1/2+(1/4+I\gamma_B/\xi^2)^{1/2}]^{-1}\exp(-E^*/kT) \qquad (10)$$

where γ_A and γ_B are the curvatures of the potential at the bottom and the top, respectively, ξ is the friction coefficient of surrounding media, E^* is the potential barrier height and $I=\Sigma m_i r_i^2$ is the moment of inertia of the rotating unit around the bond where m_i is the mass of the i-th rotating unit and r_i is the distance from the rotating axis to the i-th unit. In the molten PB system including no solvents, the observed activation energy (2.9 kcal/mol) is almost identical with one barrier height, suggesting that the effects of the friction coefficient ξ on the rate k_K is negligible. We assume that the conformational transition rate of molten PB can be described in the form of low friction limit. It is given by

$$k_K=(1/2\pi)(\gamma_A/I)^{1/2}\exp(-E^*/kT) \qquad (11)$$

Using eq.(11), we calculated the rate of the local conformational transition k_K and corresponding rest time τ_K ($=k_K^{-1}$), which are summarized in Table II. The agreement be-

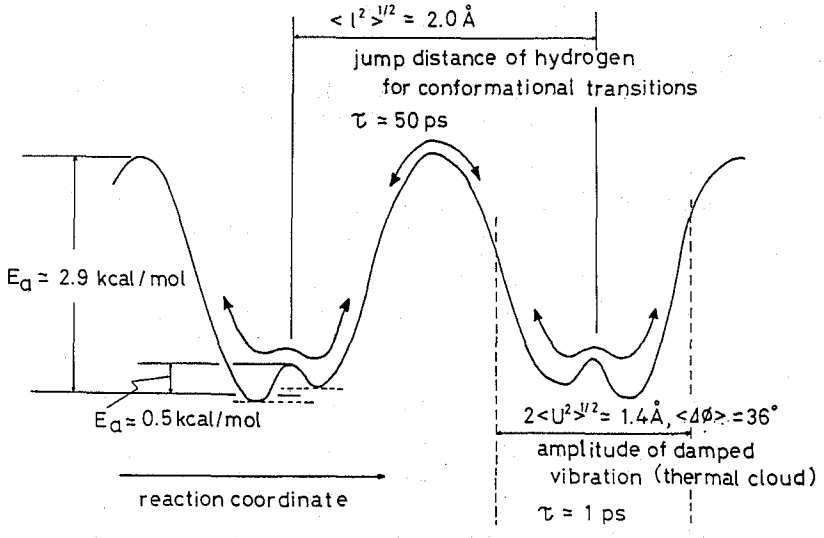

Fig. 14. Schematic potential representation for local conformational transition along the reaction coordinate.

tween τ_0 and τ_K is very good, e.g., the observed value at 100°C is 28.9 ps and the calculated one is 36.8 ps. The good agreement may offer evidence that the Kramers' rate theory at the low friction limit is appropriate for description of the local conformational transitions of the molten PB.

In conclusion, the results obtained by the jump diffusion model with the damped vibrational motions are summarized in Fig. 14 in terms of potential representation along the reaction coordinate. The physical picture of the model agrees well with the results of the computer simulation by Helfand et al. This means that polymer chains are not so hard for the conformational transitions but softened by the vibrational motions, especially by the torsional motions. The softening is essential for the conformational transitions to occur through a single bond rotation and be localized.

Furthermore, the potential picture obtained from the melt is very similar to that obtained from the analysis of the *low energy excitations* in the glassy state. It means that the "asymmetric double well potential", which is an origin of the *low energy excitation*, is a frozen state of the distorted potential in the molten state.

REFERENCES

1) For example, "Structural Studies of Macromolecules by Spectroscopic Methods", ed. by K.J. Ivin, Wiley-Interscience Publication, London, 1976.
2) P.E. Rouse, *J. Chem. Phys.*, **12**, 1272 (1953).
3) M. Doi and S.F. Edwards, *J. Chem. Soc. Faraday Trans.*, **74**, 1787, 1802, 1818 (1978).
4) For example, "Polymer Motion in Dense Systems", ed. by D. Richter and T. Springer, Springer Porceedings in Physics, 29, Springer, Berlin, 1988.
5) K. Inoue, Y. Ishikawa, N. Watanabe, K. Kaji, Y. Kiyanagi, H. Iwasa and M. Kohgi, *Nucl. Instr. Meth.*, **A238**, 401 (1984).
6) K. Inoue, T. Kanaya, Y. Kiyanagi, S. Ikeda, K. Shibata, H. Iwasa, T. Kamiyama, N. Watanabe and Y. Izumi, *Nucl. Inst. Meth.*, **A309**, 294 (1991).
7) G.E. Bacon, "Neutron Diffraction", Clarendon Press, Oxford, 1975.
8) "Amorphous Solids-Low Temperature Properties", Topics in Current Physics, 24, ed. by W.A. Phillips, Springer, Berlin, 1981.
9) T. Kanaya, K. Kaji, S. Ikeda and K. Inoue, *Chem. Phys. Lett.*, **150**, 334 (1988).
10) K. Inoue, T. Kanaya, S. Ikeda, K. Kaji, K. Shibata, M. Misawa and Y. Kiyanagi, *J. Chem. Phys.*, **95**, 5332 (1991).
11) T. Kanaya, K. Kaji and K. Inoue, *Physica B*, **181/181**, 814 (1992).
12) B. Derrida, R. Orbach and Kim-Wah Yu, *Phys. Rev.*, **B29**, 6645 (1984).
13) H.M. Rosenberg, *Phys. Rev. Lett.*, **54**, 704 (1985).
14) U. Buchenau, M. Prager, N. Nüker, A.J. Dianoux, N. Ahmad and W.A. Phillips, *Phys. Rev.*, **B34**, 5665 (1986).
15) U. Buchenau, M. Prager, W.A. Kamitakahara, H.R. Shanks and N. Nüker, *Europhys. Lett.*, **6**, 695 (1988).
16) U. Buchenau, H.M. Zhou, N. Nüker, K.S. Gilroy and W.A. Phillips, *Phys. Rev. Lett.*, **60**, 1318 (1988).
17) J. Jäkle, *Rep. Prog. Phys.*, **49**, 171 (1986).
18) J. Ferry, "Viscoelastic Properties of Polymers", Wiley, New York, 1980.
19) For example, W. Götze, "Aspects of Structural Glass Transitions" in "Liquid, Freezing and Glass Transition", ed. by J.P. Hansen, D. Leuesque and J. Zinn-Justin, North-Holland, Amsterdam, 1991.
20) For example, "Dynamics of Disordered Materials", Springer Proceedings in Physics, 37, ed. by D. Richter, A.J. Dianoux, W. Petry and J. Teixeira, Springer, Berlin, 1988.
21) T. Kanaya, T. Kawaguchi and K. Kaji, *Physica B*, in press.

22) K. Inoue, T. Kanaya, K. Kaji, Y. Kiyanagi and K. Shibata, *J. Phys. Soc. Japan*, **57**, 2862 (1988).
23) T.F. Schatzki, *J. Polym. Sci.*, **57**, 496, (1962).
24) L. Monnerie and J. Geny, *J. Chim. Phys.-Chim. Biol.*, **66**, 1691 (1969).
25) E. Helfand, Z.R. Wassermann and T.A. Weber, *J. Chem. Phys.*, **70**, 2016 (1979); E. Helfand, Wassermann and T.A. Weber, *Macromolecules*, **13**, 526 (1980).
26) T. Kanaya, K. Kaji and K. Inoue, *Macromolecules*, **24**, 1826 (1991).
27) K.S. Singwi and A. Sjolander, *J. Chem. Phys.*, **119**, 863 (1960).
28) H.A. Kramers, *Physica*, **7**, 284 (1940).